Photonic Intermediate Structures for Perovskite/c-Silicon Four Terminal Tandem Solar Cells

Augusto Martins, Ben-Hur Viana Borges, Juntao Li, Thomas F. Krauss, and Emiliano R. Martins

***Abstract*—Tandem perovskite/silicon devices are promising candidates for highly efficient and low-cost solar cells. Such tandem solar cells, however, require careful photon management for optimum performance, which can be achieved with intermediate photonic structures. Here, we identify the ideal requirements for such intermediate structures in perovskite/silicon tandem cells. Counterintuitively, we find that the reflectance in the perovskite absorption window, i.e., below approx. 800 nm wavelength, does not have a strong impact on the tandem performance. Instead, the main function of the intermediate structure is to act as an optical impedance matching layer at the perovskite–silicon interface. This insight affords the design of simple and tolerant photonic structures that can obtain efficiencies surpassing 30%, assuming a passivated emitter, rear locally diffused (PERL) bottom cell and realistic perovskite top cell, by optical impedance matching alone.**

***Index Terms*—Intermediate reflectors, optical impedance matching, perovskite, photovoltaics, photonic nanostructures, silicon, tandem solar cells.**

I. Introduction

FOR solar cells to become competitive with traditional energy sources, their cost per Watt of energy needs to be reduced. This cost depends mainly on the installation and manufacturing process as well as on the power conversion efficiency. As the average price of silicon has already dropped sharply in the last decade [1], the manufacturing costs are already very low and the installation costs are difficult to reduce, much of the research effort is now focusing on the efficiency problem. Since the efficiency of single junction silicon cells is already approaching its theoretical limit of 30% [2], [3], it is essential to seek low-cost alternatives to boost the efficiency of silicon solar cells beyond their single junction limit. As a result, there has been a surge in interest in tandem solar cells using silicon as the low band gap absorber and perovskite as the high band gap absorber [4]–[9], with the goal of exploiting the higher open-circuit voltage of perovskites. This interest is justified by the combination of the mature silicon technology with the huge potential of perovskites to deliver low-cost and highly efficient solar cells [9]–[11]. Theoretical analyses suggest that, in principle, tandem silicon perovskite cells can have efficiencies in excess of 30% [4], [5], [12], while there have been experimental reports of tandem silicon perovskite cells reaching 23.4% [6], 18% [8], 25% [13], and even 28% [14], the latter using an optical splitting system. In order to be technologically viable, tandem cells need to be realized as stacked structures, in which case the performance is highly dependent on photon management. For example, in two-terminal tandem cells, photon management is used to balance the absorption in the different layers in order to match the currents delivered by each cell. In the alternative four-terminal configuration, photon management is used to maximize the absorption in the top cell, which has the highest band gap and therefore delivers the highest open-circuit voltage ($V_{\rm oc}$). Photon management can be achieved by placing intermediate photonic reflectors between the two cells, with the reflectance designed to match the top cell absorption band. Examples of intermediate reflectors include homogeneous layers [15], [16], photonic crystals [15]–[18], metallic nanoparticles [19], stacked layers [15], [16], and a combination of those with randomly texturized surfaces [20]. It is interesting to note that most of the attention has been paid to the reflectance at shorter wavelengths, motivated by the desire to optimize the top cell performance [15]–[20], with only a few papers addressing the problem of optical impedance matching into the lower cell [18]. Here, we take the optical impedance matching concept further and demonstrate that it is, in fact, the dominant effect in determining tandem cell efficiency.

The majority of intermediate reflectors proposed so far have been targeted at micromorph solar cells, with their potential for perovskite/silicon tandem cells yet to be explored [9]. As an example of this potential, Lal *et al*. have concluded that a combination of an intermediate reflector with a Lambertian scatterer can overcome the 30% limit in a perovskite/silicon tandem

Manuscript received February 5, 2017; revised April 28, 2017; accepted May 31, 2017. Date of publication June 22, 2017; date of current version August 18, 2017. This work was supported in part by the São Paulo Research Foundation (FAPESP) under Grant #2015/21455-1 and Grant #2016/05809-0, in part by the Ministry of Science and Technology of China under Grant 2016YFA0301300, in part by the National Natural Science Foundation of China under Grant 11674402, and in part by Guangzhou Science and Technology Projects under Grant 201607010044 and Grant 201607020023. *(Corresponding authors: Juntao Li and Emiliano Rezende Martins.)*

A. Martins, B.-H. V. Borges, and E. R. Martins are with the School of Engineering of São Carlos, University of São Paulo, São Paulo 03178-200, Brazil (e-mail: augusto.martins@usp.br; benhur@sc.usp.br; erm@usp.br).

J. Li is with the State Key Laboratory of Optoelectronic Materials & Technologies, School of Physics, Sun Yat-sen University, Guangzhou 510275, China (e-mail: lijt3@mail.sysu.edu.cn).

T. F. Krauss is with the Department of Physics, University of York, York YO10 5DD, U.K. (e-mail: thomas.krauss@york.ac.uk).

This paper has supplementary downloadable material available at http://ieeexplore.ieee.org.

Color versions of one or more of the figures in this paper are available online at http://ieeexplore.ieee.org.

Digital Object Identifier 10.1109/JPHOTOV.2017.2713406

cell [12]. However, it is still not clear what the ideal properties of an intermediate structure should be and whether these properties can be met by realistic structures. Here, we address this problem by first identifying the ideal requirement for intermediate photonic structures in perovskite/silicon tandem solar cells. Importantly, and counter-intuitively, we show that the intermediate structure reflectance into the high band-gap material (perovskite) absorption window does not have a significant impact on the overall tandem performance. This conclusion differs from the requirement for micromorph solar cells [14], [21]. Instead of boosting the reflectance into the perovskite window, we show that the intermediate structure should mainly act as an optical impedance matching layer for the spectral region where the perovskite is transparent, i.e., the intermediate structure should maximize the optical transmission between the top cell and bottom cell. After carefully identifying this requirement, we design simple and robust photonic structures that provide broad-band optical impedance matching between top and bottom cells. Finally, the performance of different optical impedance matching structures is compared to that of intermediate reflectors, analyzing the impact of both classes of photonic structures on the overall performance of the tandem solar cell. The conclusion is that simple and efficient structures are obtained when only an optical impedance matching layer is used. As an example, we show that by varying the reflectivity and cut-off wavelength of the intermediate reflector, the highest increase in short-circuit current, assuming there is no light trapping, is 18.5% compared to a structure without intermediate reflector, and it is achieved for $R \approx 0$, i.e., for an optical impedance matching layer.

II. Ideal Intermediate Photonic Structure

We begin by identifying the ideal requirements for the intermediate photonic structure, which is placed between the perovskite and silicon absorbing layers of a four-terminal tandem solar cell, as shown in Fig. 1(a). The choice of a four-terminal configuration has two important advantages: 1) it does not require current matching and 2) it affords the optical separation between the top and bottom cells by means of an optical buffer. This scheme is particularly convenient because it allows the cells to be fabricated separately and be subsequently bonded together. The top cell is comprised of an antireflection (AR) coating, a 400 nm thick perovskite layer, and a 100 nm thick indium tin oxide (ITO) electrode. The top and bottom cells are optically separated by a 1 μm silicon dioxide (SiO_2) buffer, followed by the photonic intermediate structure. Finally, the cell is terminated by a 400 μm thick crystalline silicon (c-Si) absorber covered with a perfect mirror. The refractive index of the AR coating is set to 1.45 and the dispersion of all materials can be found in the Supplementary information. As the choice of the optimum transparent front contact is still under active research [22]–[26], we opted to first perform the calculations without any particular choice of front contact and transport layers, so that the results can be kept as general as possible. However, the performance characterization for a complete device using ITO as the front contact and multiple perovskite thicknesses is provided in the Supplementary information.

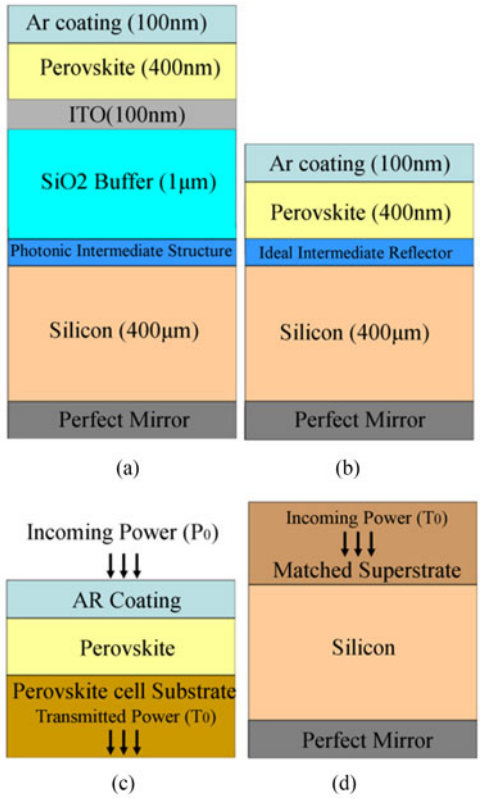

Fig. 1. (a) Intermediate photonic structure on a perovskite/c-Si tandem solar cell. The thickness of each layer is stated in parenthesis in front of the material. The refractive index of the AR coating is set to 1.45. First, the optimum properties of an ideal intermediate reflector are identified. The ideal reflector is depicted in (b). In (c), the absorption in the perovskite layer is calculated by choosing a substrate such that the Fresnel reflection coefficient between the perovskite layer and the substrate gives the desired ideal reflectance—according to the top inset of Fig. 2(a). In the second step, (d), the power transmitted into the substrate of (c) is transposed to a matched superstrate (with the same real part of refractive index as silicon), so as to avoid reflection from the silicon layer. The structure of (d) is then used to calculate the absorption in the silicon layer. The light reflected from (d) is considered as loss and does not reach (c) again.

The ideal properties of the intermediate structure can be identified by considering that an ideal reflector is placed between the perovskite and silicon layers, as shown in Fig. 1(b). The ideal reflector spectrum is shown in top the inset of Fig. 2(a): it has a fixed reflectance R_{ir} up to a cut-off wavelength λ_{irc}, after which the reflectance drops sharply to zero. The impact of the ideal reflector on the solar cell efficiency can thus be assessed by varying the reflectance R_{ir} and the cut-off wavelength λ_{irc}.

The absorption spectra of the perovskite and silicon layers in the presence of the ideal reflector are then calculated in two steps. First, the perovskite absorption and transmission are calculated by replacing the entire bottom cell, including the optical buffer, by a substrate whose refractive index is calculated from the Fresnel equations to provide the chosen reflectance R_{ir}, as shown in Fig. 1(c). Second, the power transmitted into the substrate of Fig. 1(c) is assumed to be the incident power on the matched superstrate of Fig. 1(d). Notice that the power incoming from the superstrate is the total incident power minus the power lost to both reflection and absorption in the perovskite

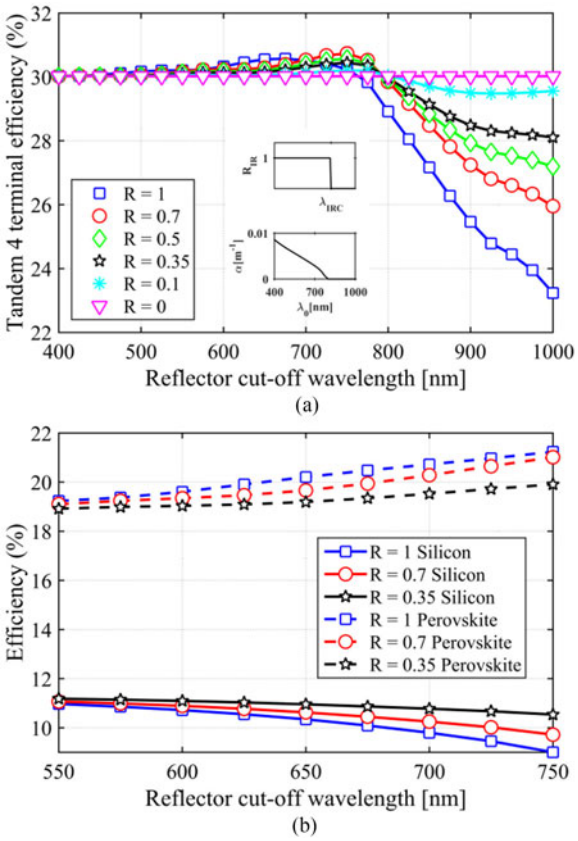

Fig. 2. (a) Dependence of the tandem solar cell efficiency on the ideal reflector cut-off wavelength. The efficiency is not strongly dependent on the reflectance for cut-off wavelengths inside the perovskite absorption window, but drops sharply for high reflectance when the cut-off wavelength reaches the perovskite transparency window. The top inset shows the reflectance of the ideal reflector and the bottom inset shows the absorption coefficient of perovskite. (b) Dependence of the silicon (continuous line) and perovskite (dashed lines) layers' efficiency on the ideal reflector cut-off wavelength.

layer. The configuration of Fig. 1(d) is then used to calculate the absorption in the silicon layer. The calculations assume perpendicular incidence and AM1.5G solar spectrum. All optical calculations were performed using the rigorous-coupled wave analysis [27].

The calculated absorptions were then used to determine the performance of the tandem cell. Following the procedure described in [4], the bottom silicon solar cell parameters are chosen based on the c-Si PERL solar cell [28]; they are: charge carrier collection probability of 0.978, fill factor of 82.8%, and open-circuit voltage $V_{\rm oc}^{\rm Si}$ given by the following diode equation:

$$V_{\rm oc}^{\rm Si} = \frac{kT}{q}\left(\frac{J_{\rm sc}^{\rm Si}}{J_0+1}\right)$$

where k is the Boltzmann constant, T is the temperature, q is the fundamental charge, $J_{\rm sc}^{\rm Si}$ is the short-circuit current density in units of mA/cm^2, and $J_0 = 4.9 \times 10^{-11}$ mA/cm^2.

The top perovskite solar cell short-circuit current, open-circuit voltage, and efficiency are also calculated according to [4]. Following [4], the parameters used in the calculations are: diffusion length $L_d = 100$ nm, luminescence efficiency of 0.55, fill factor of 80%, and band-gap of 1.55 eV. Even though the optimum band-gap is around 1.8 eV, we opted to choose a band-gap that is more similar to current perovskite materials.

Fig. 2(a) shows the tandem solar cell efficiency as a function of the cut-off wavelength $\lambda_{\rm irc}$ for different values of $R_{\rm ir}$. According to the ideal reflector spectrum [top inset of Fig. 2(a)], the reflectance between the perovskite and silicon layers is fixed to $R_{\rm ir}$ up to the cut-off wavelength. For wavelengths above $\lambda_{\rm irc}$, the ideal reflector acts a perfect optical impedance matching layer between perovskite and silicon. As perovskite absorbs up to 800 nm, it is reasonable to assume that the ideal reflector optimum parameters should be $R_{\rm ir} = 1$ and $\lambda_{\rm irc} \approx 800$ nm, since this is the condition that maximizes absorption in the high band-gap (perovskite) layer. The results of Fig. 2(a), however, contradict this assumption: it is clear that the total efficiency is not maximized for $R_{\rm ir} = 1$ and, more importantly, it depends only weakly on $R_{\rm ir}$ for $\lambda_{\rm irc}$ up to $\sim$750 nm. This counter-intuitive behavior can be explained as follows: In the wavelength region near cut-off (550 nm $< \lambda_{\rm irc} <$ 800 nm), one would expect a strong dependence of the tandem efficiency on $R_{\rm ir}$ because of the strong overlap of high solar photon density with the perovskite absorption window. According to Fig. 2(a), however, this dependence is not pronounced and, moreover, it peaks at $R_{\rm ir} = 0.7$ and $\lambda_{\rm irc} = 750$ nm instead of the expected $R_{\rm ir} = 1$, with only a weak dependence on $R_{\rm ir}$. Therefore, these results lead to the conclusion that high reflectance in the perovskite absorption window is not a strong requirement.

We propose that this counter-intuitive behavior is a consequence of the balance between reflection and thermalization losses, which is best explained by means of an example: assuming a perfect AR coating, for $R_{\rm ir} = 0$, the absorption at the wavelength of 700 nm is about 80% in the perovskite layer and 20% in the silicon layer (at this wavelength, the 400 μm thick silicon layer absorbs virtually all photons that reach it). For $R_{\rm ir} = 1$, however, and at the same wavelength of 700 nm, the absorption in the perovskite layer is about 90%, while in the silicon layer it is 0% (since no photon reaches it). This means that $R_{\rm ir} = 1$ results in higher absorption in the perovskite layer and, consequently, lower thermalization losses, yet this improvement is more than outweighed by the loss of efficiency in the silicon. Consequently, there is a trade-off between reflection and thermalization losses that cannot be overlooked in the intermediate structure design; essentially, while any value of $R_{\rm ir} > 0$ increases the absorption in the perovskite layer, it also increases the reflection back into free space, so photons are being lost rather than being absorbed in the silicon. It is this trade-off that accounts for the low dependence of the tandem efficiency on $R_{\rm ir}$ in the spectral region 550 nm $< \lambda_{\rm irc} <$ 800 nm. This compensation is clearly seen when the efficiencies for the perovskite and silicon solar cells are plotted independently [see Fig. 2(b)]: as $R_{\rm ir}$ increases, the efficiency of the perovskite top cell also increases by approximately the same amount as the efficiency of the silicon bottom cell decreases. Consequently, the tandem efficiency is not strongly affected by a change of $R_{\rm ir}$.

Even though the tandem efficiency is fairly constant for $\lambda_{\rm irc}$ up to 750 nm, the reflection loss argument starts to become much more relevant in the long cut-off wavelength region ($\lambda_{\rm irc} >$

750 nm), where the perovskite layer becomes transparent. In this region, any value of $R_{\rm ir}$ different from zero results in reflection losses, so it is of paramount importance to identify a minimum requirement for $R_{\rm ir}$. This requirement can be readily identified through the results of Fig. 2(a): it is apparent that the tandem efficiency is almost independent of wavelength for $R_{\rm ir} = 0.1$, thus indicating that the reflection losses should not be higher than 10% in the spectral region where perovskite is transparent.

We have thus gained two key insights into the analysis of the ideal intermediate reflector: 1) The device performance is almost independent of the intermediate structure reflectance in the perovskite absorption window; 2) the intermediate structure should act predominantly as an optical impedance matching layer in the spectral region where perovskite is transparent, with the requirement that the reflection arising from impedance mismatch be kept below 10%. In the next section, these insights are used to guide the design of the intermediate photonic structures.

III. Intermediate Photonic Structure Design

As discussed in Section I, we have now identified that the main role of the photonic intermediate structure in perovskite/c_Si tandem cells should be to provide optical impedance matching between the top and bottom cells. In order to better understand the role of intermediate photonic structures, we now introduce four different designs, shown in Fig. 3(a)–(d). The structures of Fig. 3(a) and (b) are designed to act as optical impedance matching layers between the top and bottom cells, whereas the structures of Fig. 3(c) and (d) are designed as intermediate reflectors. Their corresponding transmittance spectra are shown in Fig. 3(e). For reference, we also show the transmittance without any intermediate structure in Fig. 3(e). Notice that the spectra are calculated assuming incidence from the buffer SiO_2 superstrate into the silicon substrate, as required by the tandem solar cell configuration of Fig. 1(a).

Fig. 3(a) consists of only a single 80 nm thick layer of silicon nitride (Si_3N_4) sandwiched between the SiO_2 superstrate and the silicon substrate. The structure of Fig. 3(b) shows a patterned double layer photonic structure, where a 50 nm thick corrugated titanium dioxide (TiO_2) layer is combined with a homogeneous layer of the same material and thickness. The period of the TiO_2 grating is 300 nm and the fill factor is 60%. Notice that the small grating period ensures that the grating acts only as an effective medium and that there are no propagating diffraction orders. As shown in Fig. 3(e), the transmittance of the double layer structure is higher than the transmittance of the single layer structure, but the difference is not large: both structures provide broad-band high transmittance (>90%), spanning the spectral range between 500 and 1100 nm.

The intermediate structures shown in Fig. 3(c) and (d) are distributed Bragg reflectors (DBR), comprised of two and four layers, respectively. The DBRs are first optimized to provide high reflectance into the perovskite absorption spectral window and, at the same time, low reflectance in the perovskite transparency window. As a second optimization step, the DBR thicknesses were fine-tuned to optimize the overall performance of the tandem solar cell, which is discussed in detail as follows.

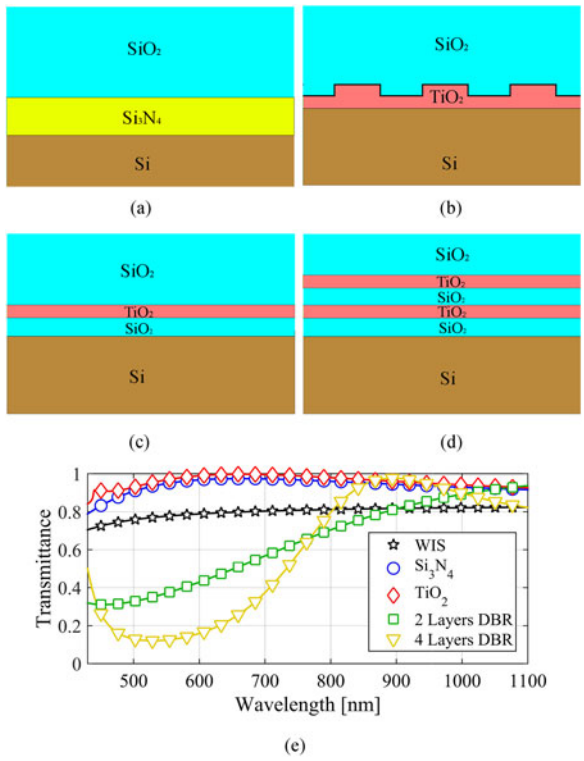

Fig. 3. (a)–(d) Four different intermediate structure designs. (a), (b) Intermediate structures designed as impedance matching layer: (a) A single 80 nm thick silicon nitride impedance matching layer. (c), (d) Intermediate structures designed as intermediate reflectors. (b) Double layer structure consisting of a corrugated TiO_2 layer, with a period of 300 nm, followed by a homogenous layer of the same material. There are no propagating diffraction orders and the grating acts only as an effective index layer. (c) A two-layer DBR with parameters fine-tuned to optimize the tandem solar cell performance. (d) A four-layer DBR with parameters fine-tuned to optimize the tandem solar cell performance. (e) Transmittance of all four intermediate photonic structures. The transmittance without any intermediate structure (WIS) is also shown for comparison. All transmittances are between the silicon dioxide superstrate and the silicon substrate.

The DBR final thicknesses are 50 nm for the TiO_2 layers and 95 nm for the SiO_2 layers.

Fig. 4(a)–(d) shows the tandem solar cells with the corresponding intermediate photonic structures, whereas Fig. 4(e) and (f) shows the absorption in the perovskite and silicon layers, respectively. As expected, the perovskite absorption is higher in the structures with intermediate reflectors, as shown in green squares and yellow triangles in Fig. 4(e). The perovskite absorption spectra for the intermediate reflectors also show more pronounced Fabry–Perot oscillations when compared to the optical impedance matching layers. We use the integrated absorption as a figure of merit to assess the performance of the structures. The integrated absorption takes into account the photon density in the solar spectrum and is defined as the total amount of absorbed solar photons divided by the total amount of incoming solar photons.

The integrated absorptions in the perovskite layer for the solar cells of Fig. 4(a)–(d) are, respectively: 46.2% (optical impedance matching), 46.2% (optical impedance matching), 49.3% (DBR), 50.2% (DBR), while the integrated absorption

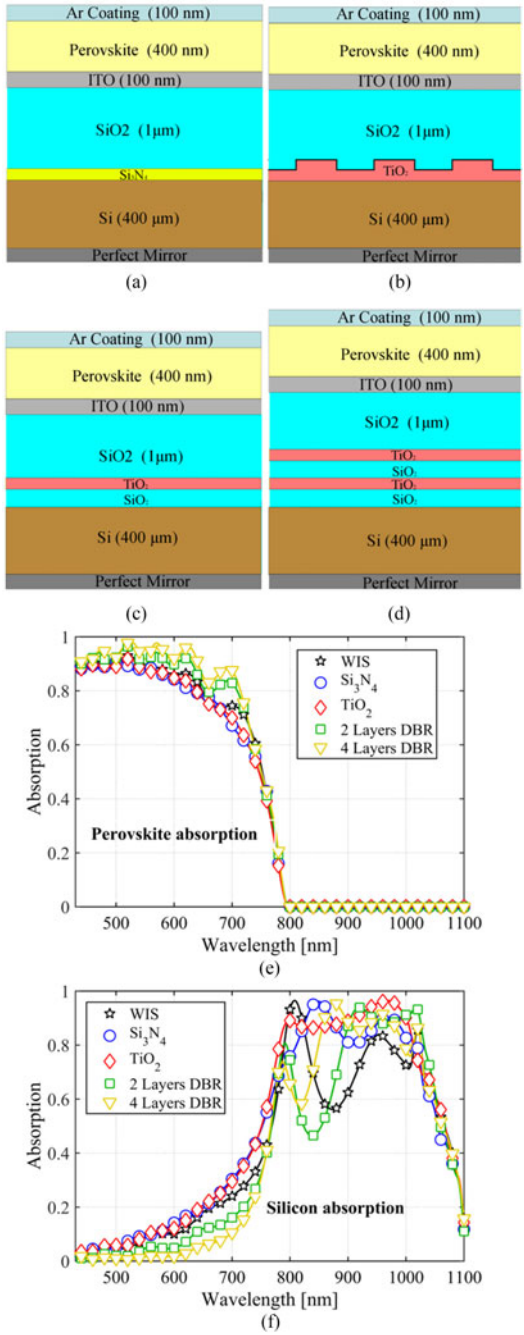

Fig. 4. (a) Illustration of the complete solar cell with the intermediate photonic structure. (a), (b) Photonic intermediate structures designed as impedance matching layers. (c), (d) Photonic intermediate structures designed as intermediate reflectors. (e) Absorption in the perovskite layer. (f) Absorption in the silicon layer.

in the perovskite layer without intermediate structure (WIS) is 47.4%. The absorption in the silicon layer shown in Fig. 4(f), on the other hand, is higher for the impedance-matched structures of Fig. 4(a) and (b).

The integrated absorptions in the silicon layer for the structures of Fig. 4(a)–(d) are, respectively: 41.9% (optical impedance matching), 43.5% (optical impedance matching), 34.6% (DBR), 34.8% (DBR), while the integrated absorption in the silicon layer WIS is 36.85%. The calculated efficiencies and

TABLE I
SOLAR CELL PARAMETERS FOR $L_d = 100$ AND 400 NM

	$L_d = 100$ nm				
	Impedance Matching layers		Intermediate Reflectors		Without intermediate structure
	Si_3N_4	TiO_2	2 Layer DBR	4 Layer DBR	
Silicon J_{sc} (mA/cm^2)	17.81	18.50	14.74	14.81	15.68
Perovskite J_{sc} (mA/cm^2)	18.79	18.79	20.05	20.57	19.29
Silicon Efficiency (%)	10.08	10.49	8.29	8.32	8.83
Perovskite Efficiency (%)	19.01	19.03	20.27	20.79	19.52
Tandem Efficiency (%)	29.09	29.52	28.56	29.11	28.35
	$L_d = 400$ nm				
	Impedance Matching layers		Intermediate Reflectors		Without intermediate structure
	Si_3N_4	TiO_2	2 Layer DBR	4 Layer DBR	
Silicon J_{sc} (mA/cm^2)	17.81	18.50	14.74	14.81	15.68
Perovskite J_{sc} (mA/cm^2)	19.98	19.98	21.32	21.87	20.50
Silicon Efficiency (%)	10.08	10.49	8.29	8.32	8.83
Perovskite Efficiency (%)	20.23	20.26	21.57	22.13	20.78
Tandem Efficiency (%)	30.31	30.74	29.86	30.45	29.61

short-circuit currents are shown in Table I for two different values of the perovskite charge carrier diffusion length: $L_d = 100$ and 400 nm.

The four-layer DBR shows high transmittance for wavelengths larger than 800 nm [see Fig. 3(e)], which results in high absorption in the silicon layer for these wavelengths [see Fig. 4(f)]. The four-layer DBR, therefore, is acting as both an intermediate reflector for the perovskite absorption window, and also as an optical impedance matching layer for wavelengths larger than 800 nm (i.e., the perovskite transparency window).

This double role of the DBR structure might justify the assumption that the four-layer DBR is the optimum structure. As shown in Table I, however, the tandem solar cell efficiency is not the highest for the four-layer DBR. Indeed, the best overall efficiency is achieved for the optical impedance matching structure comprised of the TiO_2 grating [see Fig. 4(b)]. It is important to notice that, even when compared to the simplest optical impedance matching layer [see Fig. 4(a)], the tandem efficiency of the four-layer DBR is only marginally higher. These counter-intuitive results can be understood by comparing Fig. 3(e) with 4(f): even though the transmittance for the four-layer DBR rises quickly between 700 and 800 nm; this transition is not sharp enough to mitigate reflection losses in the silicon layer. Consequently, the absorption in the silicon layer [see Fig. 4(f)] in the short-wavelength region (<850 nm) is higher for the structures that provide *only* optical impedance matching. It is this difference that accounts for the similar performances

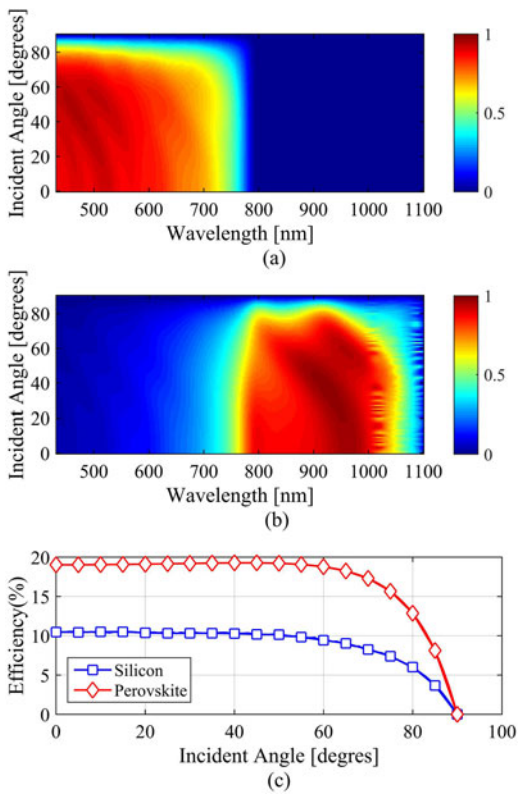

Fig. 5. Angular dependence of the solar cell performance. (a) and (b) show the absorption spectra of the perovskite and c-Si, respectively, as a function of incidence angle and wavelength. (c) Efficiency of the silicon and perovskite solar cells as a function of the incidence angle.

of the tandem solar cells, listed in Table I. These results, therefore, corroborate the previous conclusion that it is preferable that intermediate structures be designed to provide only optical impedance matching between the top and bottom cells. Indeed, the DBR intermediate structures are more complex and yet show similar performance when compared to the simplest optical impedance matching layer.

Our calculations indicate that both optical impedance matching layers result in efficiencies exceeding 30% for $L_d = 400$ nm. Naturally, we expect that the tandem device performance can be further increased by applying light trapping concepts [7], [12] and that the design of such light trapping structures will benefit from the optical impedance matching principles we have outlined here. When compared to the solar cell WIS, the silicon solar cell short-circuit current is increased by 18.5% for the TiO_2 grating. It is important to notice that these high efficiencies were achieved without any light trapping scheme, which is expected to boost the efficiencies even further [4], [12].

Resonant structures depend on specific phase accumulation requirements that tend to limit their angular performance. One additional advantage of employing optical impedance matching layers is that their nonresonant behavior results in a very angular tolerant performance. This feature can be seen in Fig. 5(a) and (b), which show, respectively, the absorption in the silicon and perovskite layers versus incidence angle (θ) and wavelength for the system with the TiO_2 grating acting as optical impedance matching layer. The dependence of the solar cell efficiencies on the incidence angle is shown in Fig. 5(c). Impressively, the efficiencies are virtually constant up to an angle of 60 degrees, implying an acceptance cone of at least 120 degrees.

IV. Summary

We have identified that a photonic intermediate structure in a perovskite/c-Si tandem solar cell should act as an optical impedance matching layer at the perovskite–silicon interface. The reason for this somewhat unexpected behavior is that by increasing the reflectivity, the reflection loss back into free space tends to outweigh the improvement in absorption in the top layer. This insight affords the relaxation of the photonic structure reflectance in the perovskite absorption window, which leads to very simple and robust designs for the intermediate structure. Accordingly, we analyze two simple designs and compare their performances with DBR-based intermediate reflectors. Our conclusion is that the intermediate structures acting only as optical impedance matching layers are much simpler than the DBR structures, yet showing similar performances. We then implement this insight by simulating a realistic device configuration and show that optical impedance matching alone can increase the short-circuit current of the silicon solar cell by 18.5% (corresponding to a boost of 2.8 mA/cm^2), thus resulting in an expected tandem efficiency in excess of 30%.

References

[1] A. Louwen, W. Van Sark, R. Schropp, and A. Faaij, "A cost roadmap for silicon heterojunction solar cells," *Sol. Energy Mater. Sol. Cells*, vol. 147, pp. 295–314, 2016.
[2] P. K. Nayak and D. Cahen, "Updated assessment of possibilities and limits for solar cells," *Adv. Mater.*, vol. 26, pp. 1622–1628, 2014.
[3] M. A. Green, K. Emery, Y. Hishikawa, W. Warta, and E. D. Dunlop, "Solar cell efficiency tables (version 47)," *Prog. Photovolt.: Res. Appl.*, vol. 24, pp. 3–11, 2016.
[4] T. P. White, N. N. Lal, and K. R. Catchpole, "Tandem solar cells based on high-efficiency c-Si bottom cells: Top cell requirements for >30% efficiency," *IEEE J. Photovolt.*, vol. 4, no. 1, pp. 208–214, Jan. 2014.
[5] M. Filipič *et al.*, "CH3NH3PbI3 perovskite/silicon tandem solar cells: Characterization based optical simulations," *Opt. Express*, vol. 23, pp. A263–A278, 2015.
[6] R. Sheng *et al.*, "Four-terminal tandem solar cells using CH3NH3PbBr3 by spectrum splitting," *J. Phys. Chem. Lett.*, vol. 6, pp. 3931–3934, 2015.
[7] D.-L. Wang *et al.*, "Highly efficient light management for perovskite solar cells," *Sci. Rep.*, vol. 6, 2016, Art. no. 18922.
[8] S. Albrecht *et al.*, "Monolithic perovskite/silicon-heterojunction tandem solar cells processed at low temperature," *Energy Environ. Sci.*, vol. 9, pp. 81–88, 2016.
[9] O. Graydon, "The race for tandems," *Nature Photon.*, vol. 10, pp. 754–755, Dec. 2016.
[10] G. Hodes, "Perovskite-based solar cells," *Science*, vol. 342, pp. 317–318, 2013.
[11] Y. Li *et al.*, "High-efficiency robust perovskite solar cells on ultrathin flexible substrates," *Nature Commun.*, vol. 7, 2016, Art. no. 10214.
[12] N. N. Lal, T. P. White, and K. R. Catchpole, "Optics and light trapping for tandem solar cells on silicon," *IEEE J. Photovolt.*, vol. 4, no. 6, pp. 1380–1386, Nov. 2014.
[13] J. Werner *et al.*, "Efficient near-infrared-transparent perovskite solar cells enabling direct comparison of 4-terminal and monolithic perovskite/silicon tandem cells," *ACS Energy Lett.*, vol. 1, pp. 474–480, 2016.
[14] H. Uzu *et al.*, "High efficiency solar cells combining a perovskite and a silicon heterojunction solar cells via an optical splitting system," *Appl. Phys. Lett.*, vol. 106, 2015, Art. no. 013506.

[15] A. Bielawny, C. Rockstuhl, F. Lederer, and R. B. Wehrspohn, "Intermediate reflectors for enhanced top cell performance in photovoltaic thin-film tandem cells," *Opt. Express*, vol. 17, pp. 8439–8446, 2009.
[16] P. G. O'Brien *et al.*, "Photonic crystal intermediate reflectors for micromorph solar cells: A comparative study," *Opt. Express*, vol. 18, pp. 4478–4490, 2010.
[17] A. Bielawny *et al.*, "3D photonic crystal intermediate reflector for micromorph thin-film tandem solar cell," *Phys. Status Solidi A*, vol. 205, pp. 2796–2810, 2008.
[18] S. Fahr, C. Rockstuhl, and F. Lederer, "Sandwiching intermediate reflectors in tandem solar cells for improved photon management," *Appl. Phys. Lett.*, vol. 101, 2012, Art. no. 133904.
[19] S. Fahr, C. Rockstuhl, and F. Lederer, "Metallic nanoparticles as intermediate reflectors in tandem solar cells," *Appl. Phys. Lett.*, vol. 95, 2009, Art. no. 121105.
[20] S. Fahr, C. Rockstuhl, and F. Lederer, "The interplay of intermediate reflectors and randomly textured surfaces in tandem solar cells," *Appl. Phys. Lett.*, vol. 97, 2010, Art. no. 173510.
[21] T. Todorov, O. Gunawan, and S. Guha, "A road towards 25% efficiency and beyond: Perovskite tandem solar cells," *Mol. Syst. Des. Eng.*, vol. 1, pp. 370–376, 2016.
[22] P. Löper *et al.*, "Organic–inorganic halide perovskite/crystalline silicon four-terminal tandem solar cells," *Phys. Chem. Chem. Phys.*, vol. 17, pp. 1619–1629, 2015.
[23] G. E. Eperon, V. M. Burlakov, A. Goriely, and H. J. Snaith, "Neutral color semitransparent microstructured perovskite solar cells," *ACS Nano*, vol. 8, pp. 591–598, 2014.
[24] C. Roldán-Carmona *et al.*, "Flexible high efficiency perovskite solar cells," *Energy Environ. Sci.*, vol. 7, pp. 994–997, 2014.
[25] Z. M. Beiley *et al.*, "Semi-transparent polymer solar cells with excellent sub-bandgap transmission for third generation photovoltaics," *Adv. Mater.*, vol. 25, pp. 7020–7026, 2013.
[26] G. Y. Margulis *et al.*, "Spray deposition of silver nanowire electrodes for semitransparent solid-state dye-sensitized solar cells," *Adv. Energy Mater.*, vol. 3, pp. 1657–1663, 2013.
[27] D. M. Whittaker and I. S. Culshaw, "Scattering-matrix treatment of patterned multilayer photonic structures," *Phys. Rev. B*, vol. 60, pp. 2610–2618, 1999.
[28] J. Zhao, A. Wang, M. A. Green, and F. Ferrazza, "19.8% efficient "honeycomb" textured multicrystalline and 24.4% monocrystalline silicon solar cells," *Appl. Phys. Lett.*, vol. 73, pp. 1991–1993, 1998.

Authors' photographs and biographies not available at the time of publication.